ELSEVIER

R113 Boiling heat transfer modeling on porous metallic matrix surfaces

G. N. Danilova and A. V. Tikhonov
Heat and Mass Transfer Department, St. Petersburg State Academy of Refrigeration and Food Technologies, St. Petersburg, Russia

An experimental method for simulating fibermetal and screen surfaces by winding several layers of thin wire on the tube is proposed, temperature field measurements across the height of a layer appearing possible. Tests were carried out for R113 boiling at atmospheric pressure and for heat fluxes from 7 kW/m^2 to 100 kW/m^2. Test results, including heat transfer coefficients and temperature fields, are presented. These are interpreted qualitatively.

Keywords: porous coating; pool boiling; experimental model; temperature field across porous layer

Introduction

Published experimental investigations of processes occurring within a thin porous layer are rarely found in the literature on enhanced boiling heat transfer (Nikayama et al. 1980; Chyu and Fei 1990). However, it is these processes that define heat transfer during boiling on such surfaces. Moreover, no papers with experimental measurements of temperature fields inside a surface layer have been brought out. Such test data would permit researchers to trace the influence of porous or structured layer geometries on temperature fields and to analyze the mechanism of enhanced heat transfer.

The authors have tried to model fibermetal porous coatings using several thin layers of wire wound on a tube. Use of such a coating, which is similar to fibermetal and screen coatings, porosity and width might easily be calculated.

The authors believe that temperature measurement across the porous layer is the main advantage of the proposed test model, because each layer of a lacquered wire is a thermal resistance at the same time, and, when calibrated, mean temperatures of particular layers can be read during boiling. The thermal resistance of a very thin lacquer layer laid on the wires for electrical insulation is somewhat equal to that of an oxidized layer that forms on every fiber during manufacturing of actual fibermetal or screened coating.

Experimental rig and procedure

In a vessel with heaters and condenser, saturated R113 boils on a tested model surface with a porous coating. The design of the vessel is typical of pool-boiling tests. Figure 1a shows the experimental rig and the test cell being used with the proposed technique.

The heaters and the condenser are connected with two thermostats, which help to provide the saturated state of a tested liquid. Glass windows permit visual observations of the boiling process. The pressure was measured by reference manometer.

The test element (Figure 1b) is a copper tube with several copper wire layers wound on it. The electric wire heater enclosed in a quartz tube inside the copper tube heats the surface tested. The temperature of the copper tube surface is read by means of a thermocouple that is a constantan film vacuum-sprayed on copper tube patches. The uncoated part of the tube is electrically insulated by photoresistor before spraying the film. The constantan film does not cover the entire surface of the tube. The advantages of this temperature sensor are the possibility of mean surface temperature measurements and their high reliability, because the film width is very small (less than 5 μm), as is the area it covers (approx. 12% of total heated surface). Because of this, the film does not greatly affect vapor generation. The film thermocouple was connected to the measuring system by two leads: copper and constantan wires. One end of copper lead was minted in the surface of copper tube, and the end of constantan lead was thoroughly pressed to the constantan film using a special teflon ring and a screw. The bare tube with the film thermocouple is shown in Figure 1c. The leads of both copper wires–thermoresistors and the thermocouple are passed through a gasket and then to the ohmmeter and the millivoltmeter.

Test surfaces were hand-made and geometrical parameters were measured with a microscope. After manufacturing, the electrical insulation between each layer and tube surface was controlled.

The film copper–constantan thermocouple and thermoresistor copper wires were calibrated, using a reference platinum thermoresistor, for the temperature range to be tested. Special equipment for calibration of non standard sensors was manufactured (Figure 1d). A massive electrically heated copper cylinder with two drilled holes was thoroughly thermally insulated. In one hole, the tested tube with the film thermocouple and the porous layer

Address reprint requests to Prof. G. N. Danilova, Heat and Mass Transfer Department, St. Petersburg State Academy of Refrigeration and Food Technologies, Lomonosova, 9, St. Petersburg, 191002, Russia.

Received 22 September 1994; accepted 28 July 1995

Int. J. Heat and Fluid Flow 17: 45–51, 1996

655 Avenue of the Americas, New York, NY 10010

0142-727X/96/$15.00
SSDI 0142-727X(95)00071-W

made of wound wires was located, and in the other hole the reference platinum thermoresistor was placed. Steady-state regime for different temperature values was provided during calibration. Readings of tested sensors and reference platinum thermoresistor were measured, and after processing, graduation curves for tested sensors were derived. During the tests, the electrical resistances were measured with the help of the digital ohmmeter SH-34, that provided precise measurements of electric resistance (error less than 0.1%).

The uncertainty analysis shows that temperature measurements might be done with accuracy not worse than 0.5%; heat flux density measurements, 5%; all geometric measurements, 1%. Measurement of α might be done with accuracy not worse than 5%. The experimental method suggested permits us to measure temperature across modeled porous coatings, as well as their boiling heat transfer coefficients.

Calculation of the test surface geometries

The layer porosity ε is calculated on the basis of a geometrically simplified structure. The porosity is one of the main characteristics of porous coatings. Different test data are usually compared between themselves according to the value of ε.

The total layer volume V_l is found from the expression

$$V_l = \left[\pi(D + 2\delta_m)^2/4 - \pi D^2/4\right] \tag{1}$$

where D is the tube diameter, and δ_m is the thickness of the porous coating.

The volume of each layer $V_{w,i}$ is

$$V_{w,i} = \pi\left(D + (2i-1)d_w\right)n_i \pi d_w^2/4 \tag{2}$$

where d_w is the diameter, i is the number of layers (from 1 to n, where the first is the nearest to the copper tube surface) and n_i is the density of wire turns.

Then

$$\varepsilon = \left(V_l \sum_i^n V_{w,i}\right)/V_l \tag{3}$$

Effective diameter d_{eff} is the calculated mean diameter of a pore for the assumed geometrical model of the porous layer. The value of d_{eff} might enable us to compare the different porous structures, because it characterizes the permeability of the layer.

To calculate d_{eff}, let us consider an ideal model. Assume that all wire layers are arranged uniformly, crossing perpendicularly, and all fibers lie normally to the heat flux vector in the plane. The model can be arranged as shown in Figure 2. To define the correlation between d_{eff}, d_w, and ε for this structure, let us also examine the element from the coating. For the assumed fiber arrangement, each layer seems to replicate a previous one, being turned only by an angle of 90°. Therefore, regardless of the layer width, the effective diameter of a pore will not change. Study of the works of Dulnev et al. (1968), Dulnev et al. (1974), and Semena et al. (1984), where the relation $d_{\text{eff}} = f(\varepsilon, d_w)$ was analyzed, proved this assumption, the latter being known to have been used as a background by many workers. To find parameters of the element the volumes of wires and spaces are defined. This allows us to find d_{eff} (Figure 2a,b). The transformation will result in the following expression for an effective diameter.

$$d_{\text{eff}} = \frac{d_w}{2(1-\varepsilon)}(\pi\varepsilon)^{0.5} \tag{4}$$

This dependence differs slightly from that for fibermetal coating, which results from a more regular arrangement of wires in comparison with fibers.

Notation

A	coefficient, $A = \pi^{0.5}$ $[\beta/(1-\beta)]$ $[1/(1-\beta)$ $ln(1/\beta) - 1]$
a_c	calculated wire parameter, m; $a_c = (\pi/4)^{0.5} d_c$
b_{lr}	calculated wire parameter, m; $b_{lr} = (\pi/4)^{0.5}\delta_{lr}$
D	diameter of a tube, m
D_o	outside diameter of coated tube, m; $D_o = D + 2d_w n$
d_w	wire diameter, m; $d_w = d_c + 2\delta_{lr}$
d_c	diameter of copper core of a wire, m
d_{eff}	effective diameter of a pore, m
F_b	square area of a bare tube, m^2
F_i	square area of ith wire layer, m^2
m	molecular weight, kg/kmole
M	correction for nonideal thermal contact; $M = y + [2A(1-y^2)^{0.5}(1-y)]/[2(1-y^2)^{0.5} + (1-y)]$
n	number of layers
n_i	density of turns for ith layer, m^{-1}
p	pressure, bar
R	thermal resistance, m^{2}K/W
R_z	surface roughness, μm
q	heat flux, W/m^2
q_{lin}	linear heat flux, W/m
t	temperature, °C
$t_{w,i}$	temperature of ith wire layer, °C
T_{cr}	critical temperature, K
V_l	overall porous layer volume, m^3
$V_{w,i}$	ith wire layer volume, m^3
y	relative dimension of contact spot between wires

Greek

α	heat transfer coefficient, W/(m^{2}K)
β	heat conductions ratio, $\beta = \lambda_{\text{lq}}/\lambda_m$
δ	thickness, m
ε	porosity of a layer
λ	heat conductivity, W/(mK)
ψ	coefficient allowing for the part of a surface involved into boiling heat transfer

Subscripts

c	material of a wire (copper)
cal	calculated
cr	critical point
eff	effective parameter
l	layer
lq	liquid
lr	lacquer electrical insulation
m	porous matrix
p · b	pool boiling
s	saturation
w	wire
wall	tube wall

Superscripts

out	outer
t	test

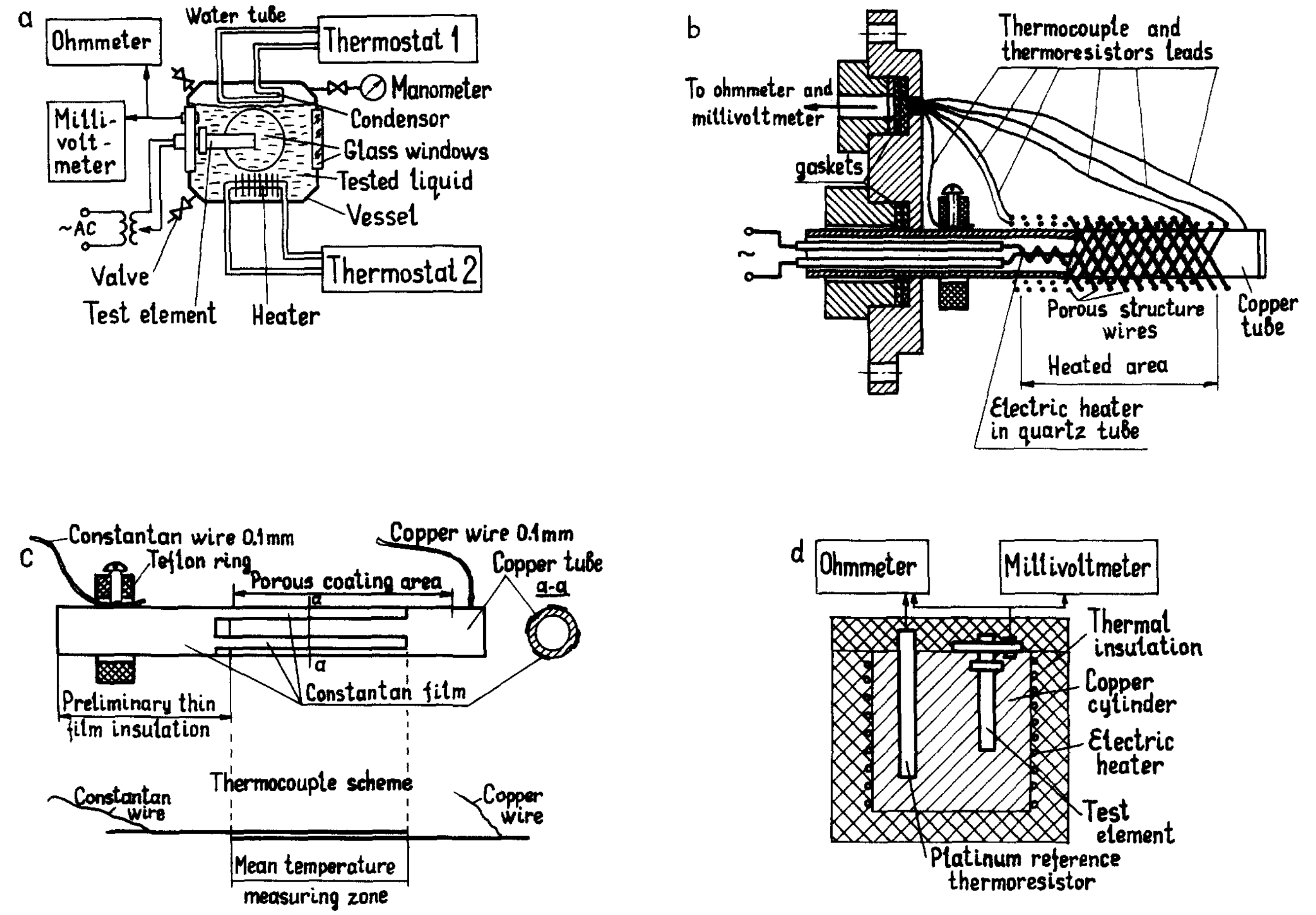

Figure 1 (a) the experimental rig; (b) the test cell simulating a tube with a porous (fibermetal or screen) coating (c) the film thermocouple; and (d) the testing rig for sensors calibration

Analysis of different equations for calculating effective heat conductivity of complex structures containing a matrix, made of a high-heat conductivity material, favors selection of the most suitable (the authors believe) equation for this case (Semena et al. 1984). This equation was derived especially for fibermetal and screen coatings and was experimentally proved for them.

$$\lambda_{\text{eff}} = \lambda_m \left[(1-\varepsilon)^2 M + \varepsilon^2 \beta + 4\beta\varepsilon \frac{1-\varepsilon}{1-\beta} \right]$$

$$M = y + \left[2A(1-y^2)^{0.5}(1-y) \right] / \left[2(1-y^2)^{0.5} + (1-y) \right] \tag{5}$$

where M is the correction for nonideal thermal contact, and y was assumed to be 0.05, according to Semena et al. (1984).

$$A = \sqrt{\pi}\,\frac{\beta}{1-\beta}\left(\frac{1}{1-\beta}\ln\frac{1}{\beta} - 1\right),\ \beta = \lambda_{lq}/\lambda_m$$

Thermal resistance of the lacquer layer must be allowed for when effective heat conductivity for the structure with electrically lacquer-insulated wires wound on the copper tube is being calculated. In this case, the model for calculation of λ_{eff} makes an additional assumption: the square area of the lacquered wire section is substituted by that of a coated square bar (Figure 2c).

It is necessary to show the difference of calculating λ_{eff} from Semena et al. (1984). The thermal resistance schema of the capillary structure is given in Figure 2d. The model of a two-component fiber is also presented. The thermal resistance of the square bar in lacquered electrical insulation R_m will be the sum of thermal resistances.

$$R_m = R_{lr} + R_c + R_{lr} \tag{6}$$

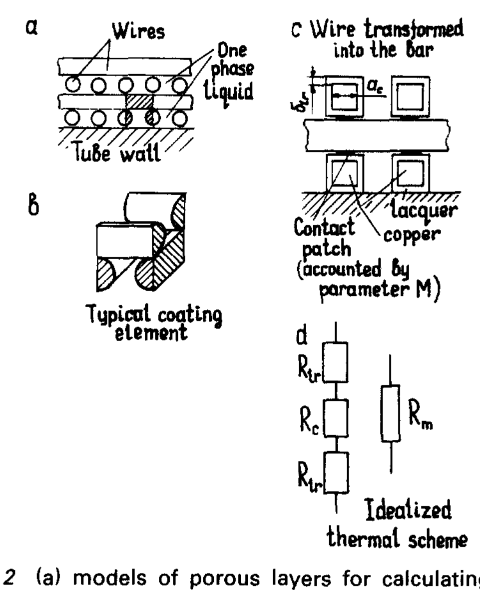

Figure 2 (a) models of porous layers for calculating of the effective diameter of a pore d_{eff}; and (b, c, d) effective heat conductivity coefficient λ_{eff}

where R_{lr} is the thermal resistance of lacquer insuation, and R_c is the thermal resistance of a square copper bar.

Hence

$$\lambda_m = (a_c + 2\delta_{lr})/(2\delta_{lr}/\lambda_{lr} + a_c/\lambda_c) \tag{7}$$

where δ_{lr} is the thickness of lacquer insulation, λ_{lr} is the lacquer thermal conductivity, λ_c is copper thermal conductivity, a_c and d_w are correlated by the following equation

$$a_c = (\pi/4)^{0.5}(d_w - 2\delta_{lr}) \tag{8}$$

The λ_m obtained is used in calculation of λ_{eff}. Using Equation 5, the values of λ_{eff} for the wire-wound porous coatings are given in Table 1.

The authors believe that the calculated values of λ_{eff} might be useful for comparing these modeled surfaces.

Test results and analysis for R113 boiling on modeled coated surfaces

In the tests performed, λ^t_{eff} values for porous layers were measured at boiling. Those values were found using measured temperatures of the outer wire layer and the tube surface according to Equation 9.

$$\lambda^t_{eff} = \frac{q_{lin} \ln[(D_0 - d_w)/D]}{2\pi(t_{wall} - t^{out}_w)} \tag{9}$$

where q_{lin} is linear heat flux density, and t^{out}_w is the axial temperature of the nth outer wire layer.

Boiling heat transfer coefficients were calculated from Newton–Rikhmann's law.

$$\alpha = q/(t_{wall} - t_s) \tag{10}$$

where wall temperature t_{wall} was read from the copper–constantan film thermocouple; whereas, t_s was from the saturated pressure.

The aims of the tests were: (1) to study wire diameter effect on boiling heat transfer; and (2) to measure temperature across the layers with different thicknesses, porosities, and wire diameters.

Tests were carried out for pool boiling of saturated R113 at atmospheric pressure on bare and porous tubes with modeled layers. Porous coatings modeled by wound copper wires are characterized in Table 1.

The values of experimentally defined λ^t_{eff} divided by the calculated value of λ_{eff} (from Table 1) are given in Figure 3. We can see that during boiling, $\lambda^t_{eff}/\lambda_{eff}$ lies between 1.6 and 2.9. Unfortunately, it is impossible to compare λ^t_{eff} with data in the literature, because the latter concern cases for matrices filled with one-phase liquids.

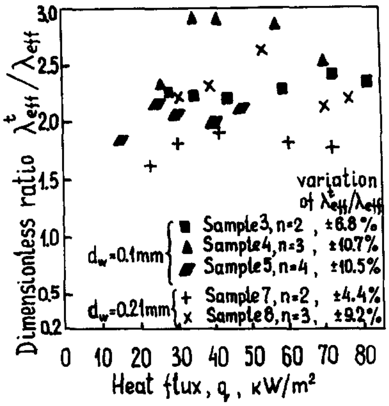

Figure 3 Effect of heat flux on the value of ratio $\lambda^t_{eff}/\lambda_{eff}$

Notice that effective conductivity λ^t_{eff} usually does not vary significantly with q (except at $q = 53$ kW/m^2 for porous coating made of three diameter 0.21-mm wire layers). This might show that at high heat fluxes, a porous layer filled with a boiling liquid impedes rapid α grouth. For surfaces with coatings made of more then two wire layers, degradation of heat transfer coefficient when q exceeds 40 kW/m^2 is confirmed by Figure 7. Thermal resistance of such a layer limits the performance of porous coated surfaces.

The test data q *versus* Δt for modeled surfaces are presented in Figure 4. Performance is known to increase for small temperature differencies; this is typical of other enhanced surfaces. It should be mentioned that the heat transfer coefficient is inversely proportional to the thermal resistance, calculated for a layer (Figure 5).

The thermal conductivity δ_m/λ_{eff} for samples 6 and 7, whether or not filled with boiling liquid, is less than for samples 3, 4, and 5. Therefore, boiling performance of surfaces with coatings made of thick wire (the former samples) will be higher than for the latter samples.

The test results processed in a form of α *versus* δ_m/d_w or n for nearly constant heat fluxes are shown in Figure 6. The authors think that optimal value of the ratio δ_m/d_w lies between one and two; when q increases, the ratio is decreasing. This might be attributable to better vapor transport for coatings with small values of δ_m/d_w. Capillary channels formed in this way will have simpler geometry, and no vapor trapping will occur.

The test data in Figure 7 processed as α *versus* q allow us to see the effect of porous layer thickness on heat transfer. Performance increase with heat flux increase occurs for all samples for q less than 20 kW/m^2. Hence, for higher q, α increases only for the layers with small δ_m/d_w, and only for samples 2, 3, and 6, α

Table 1 Description of surfaces

Designation	n of a sample	Wire diameter of coating, mm	Number of wire layers	δ_m, mm	$\frac{\delta_m}{\lambda_{eff}} \cdot 10^3$, m^{2}K/W	ε, %	d_{eff}, mm	λ_{eff}, W/m^{2}K
○	1	Bare surface (copper)						
Surfaces with modeled porous coating (copper)								
●	2	0.1	1	0.1	0.33	60	0.172	0.3
■	3	0.1	2	0.2	0.51	52	0.133	0.39
▲	4	0.1	3	0.3	0.79	53	0.137	0.38
■	5	0.1	4	0.4	0.91	48	0.118	0.44
*	6	0.21	1	0.21	0.26	54	0.297	0.813
+	7	0.21	2	0.42	0.41	48	0.248	1.011
×	8′	0.21	3	0.63	0.65	49.3	0.258	0.966

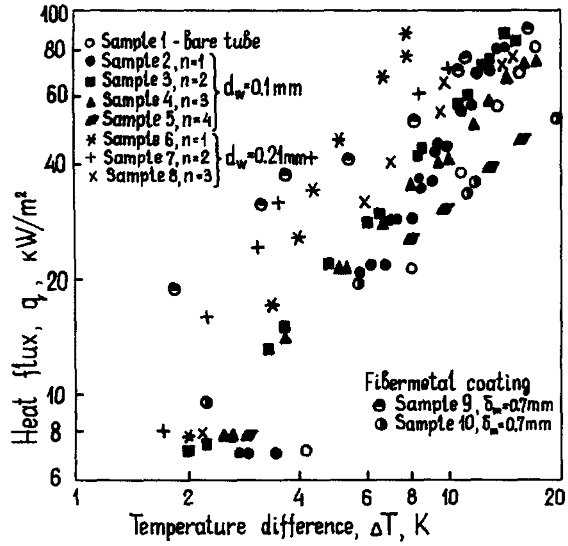

Figure 4 Boiling R113 test results for modeled surfaces and for real fibermetal surfaces

increases the entire region of q tested. Layer thicknesses of these samples do not exeed 0.21 mm. Vapor trapping of porous layers occurs for the surfaces with δ_m/d_w more than 2 and q usually more than 50 kW/m^2. Vapor trapping was found to result in worse performances of samples 4 and 5 than of bare surfaces.

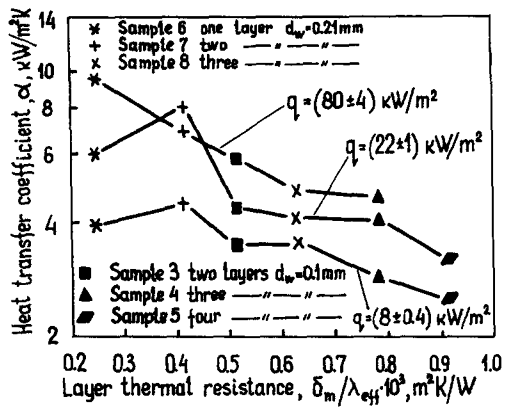

Figure 5 Dependence α *versus* thermal resistance (δ_m/λ_{eff})

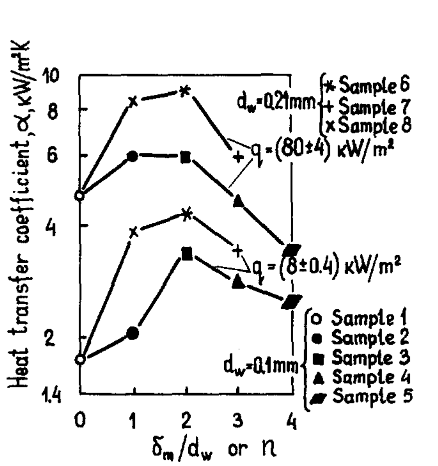

Figure 6 Effect of reduced thickness (δ_m/d_w) on heat transfer coefficient α

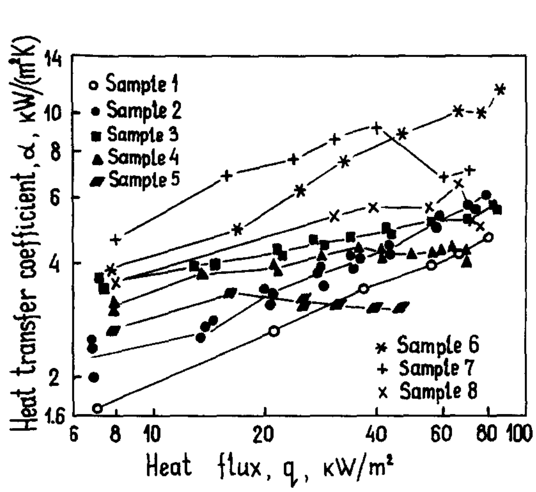

Figure 7 Heat transfer performance *versus* heat flux for R113 boiling on modeled surfaces

When the the results of tests were analyzed, it was noticed that boiling on modeled surfaces was similar to the process on the fibermetal and screen-coated surfaces (Semena et al. 1992). The following facts prove this: (1) absence of explicit change in boiling heat transfer performance at relatively high heat fluxes; and (2) presence of two stages of boiling. For small q, a significant increase of α is observed, and for higher q, the performance is constant or even decreases.

The test results of R113 boiling at normal pressure on fibermetal surfaces (Tikhonov and Zaporozhtchenko 1984) are presented in Figure 4. The characteristics of samples 9 and 10 are as follows: δ_m is 0.7 mm; ε is 0.5 and 0.6, respectively; and the fiber diameter is 0.03 mm. From Figure 4, it can be seen that the test results for modeled and real coatings agree well.

The temperature measurements across the height of modeled coatings for samples 3, 4, and 5 are shown in Figure 8. For sample 3 with high boiling performance, the whole porous layer was well heated, and temperatures of the wire layers were nearly equal. The coatings with three and four wire layers are characterized by considerable temperature differences across the layers, with high temperature of the first wire layer, and those of the third and forth layers nearly equal to t_s. Hence, only a thin wall layer was observed to be active in heat transfer, while the outer layers only resisted resultant vapor.

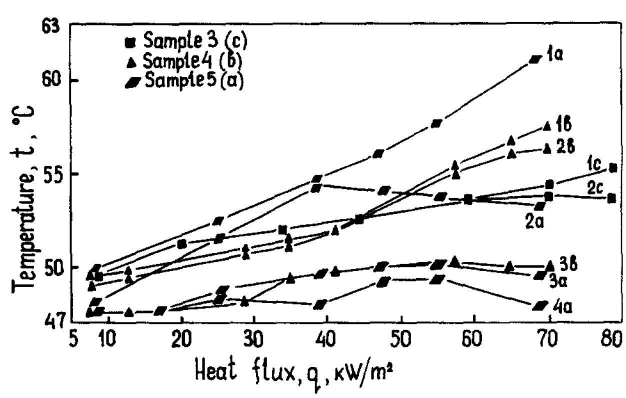

Figure 8 Temperature profiles with experimental dots across the thickness of a modeled porous layer: (a) sample 5; (b) sample 4; (c) sample 3; number on the figure corresponding to numbers of the wire layers; i.e., 1c – temperature of the first layer of the Sample $n3$

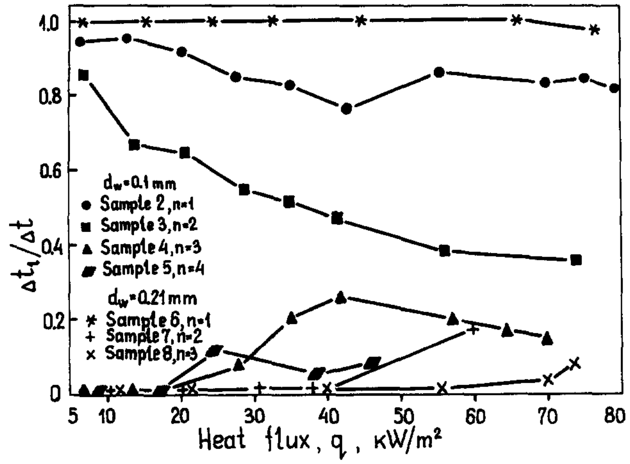

Figure 9 Dependence $\Delta t_l/\Delta t$ *versus* heat flux q

Layer thickness effect may be made clearer if the test results are processed as follows:

$$\frac{\Delta t_l}{\Delta t} = \frac{t_w^{(n)} - t_s}{t_{\text{wall}} - t_s} = f(q) \tag{11}$$

In this case, it is necessary to trace which part of temperature difference is contributed by the porous layer and how it is connected with q (Figure 9). It became clear that there were very small temperature differences across porous layers for the most effective samples 2, 3, and 6; i.e., temperatures of the matix were nearly equal to the tube's wall temperatures.

Discussion

After analyzing the test results, the authors attempted to explain heat transfer enhancement attributable to surface increase. The calculated heat flux q_{cal} from the enhanced tube was compared with q_t measured in the tests. The value of q_{cal} was defined according the following equation:

$$q_{\text{cal}} = \left[F_b \psi \alpha_{p,b}(t_{\text{wall}} - t_s) + \sum_i^n F_i \psi \alpha_{p\cdot b}(t_{w,i} - t_s) \right] / F_b \tag{12}$$

where F_b is the heated square of a bare tube, F_i is the square of ith layer of wound wire, and ψ is assumed to be 0.9 and to characterize the part of the surface involved in boiling heat transfer.

Pool-boiling heat transfer coefficient $\alpha_{p\cdot b}$ was calculated according to the Danilova (1968) equation:

$$\alpha_{p\cdot b} = C_0 F(P/P_{\text{cr}}) q^{0.75} (R_z/R_{z0})^{0.2}$$

where $C_0 = 550 P_{\text{cr}}^{0.25} T_{\text{cr}}^{-0.875} m^{-0.125}$: P_{cr} and T_{cr} are pressure and temperature at critical point: m is the molecular weight, $F(P/P_{\text{cr}}) = 0.14 + (P/P_{\text{cr}})[1.6 + 0.4/(1 - P/P_{\text{cr}})]$, R_z is the surface roughness, $R_{z0} = 1$ μm, $F(P/P_{\text{cr}})$, according to Haffner (1970).

The temperatures of wires and tube wall were taken from the test data. In Table 2, the results of comparison are presented. We can see that for heat fluxes higher than 24, kW/m^2, q_{cal} differs from q_t significantly. But for q less than 24, kW/m^2, q_{cal} and q_t are comparable, and increase of the performance may be explained by heat transfer surface increase. Such a character of heat transfer might be explained by existence of two boiling regimes.

Primarily, q increase caused vapor filling of porous matrix, but not intensive enough to fill the coating with vapor. It might be supposed that boiling occurs in that fashion on bare surfaces, and all the surface of a matrix participates in the process. For this stage, α increase may be explained by total surface increase.

During the second stage of boiling, vapor generation exceeds such a level, so that the porous matrix is saturated with vapor and most of the surface does not participate in heat transfer. Here, we should mention layer transport quality. For the thick wire structure with 0.21 mm diameter, ratio q_{cal}/q_t was 1.23 at $q \sim 77$ kw/m^2 and for wires with 0.1 mm diameter, the same ratio was 1.90, other conditions being equal. The authors believe that a porous matrix made of thin wires can be saturated with vapour, and it becomes unsuitable for vapor transport at high heat fluxes. For this stage, surface increase does not cause the rise of the performance.

To conclude, vapor transport performance of a surface with porous layer may be determined not only by geometry, but also by fluid flow inside a layer. For any type of a surface, this factor plays a key role at relatively high heat fluxes. The vapor generation process inside the enhanced structure is limited by vapor transport performance. The heat transfer mechanism considered above explains the fact that, for very high q for most types of surfaces, including fibermetal and screen ones, heat transfer performance decreases and is nearly equal to α on bare surfaces.

Conclusions

The method suggested for experimental modeling of porous layers with regular screen or fibermetal structures permits us: (1) to find accurate geometry parameters for porous layers and to estimate their effect on heat transfer performance; and (2) to monitor the temperature field across the height of a layer. Temperature fields measured may be helpful for describing boiling mechanism inside porous matrices.

The test data of R113 boiling on modeled surfaces were found to agree with results observed on actual fibermetal coatings (Tikhonov and Zaporozhtchenko 1984). Satisfactory qualitative identity of boiling processes should be mentioned; i.e., enhancement of heat transfer for small q and thin layers and degradation of the performance at high q and for thick layers.

The factor limiting heat transfer performance of fibermetal or any other type of enhanced surfaces is likely to be fluid flow and thermal resistance of porous layer, filled with two-phase refrigerant. The analysis of actual processes seems to be more accurate, if the temperature field of wall layer is known, and the behavior of surface boiling is filmed.

Table 2 Comparison of q_t and q_{cal}, Equation 12

n of sample		5					8		
q_{cal}	W/m^2	1440 *	11,150	22,300	78,000	170,000	19,100	47,800	76,400
q_t	W/m^2	7800	9550	17,500	41,400	63,700	16,000	35,000	62,100

* Calculated with assumption $\alpha = 200$ W/m^{2}K as for free convection, because temperature difference was very small for the beginning of pool boiling on a bare surface; that is the only case where q_{cal} was less than q_t.

References

Chyu, M. C. and Fei, T. 1990. Boiling heat transfer from vertical wall subjected to an inclined wall attachment. *Exp. Thermal and Fluid Science*, **3**, 256–263

Danilova, G. N. 1968. Boiling heat transfer of refrigerants. D. S. thesis, LTIHP, St. Petersburg, Russia (in Russian)

Dulnev, G. N. and Zarichnyak, U. P. 1974. *Thermal Conductivity of Mixtures and Compound Materials*. Energia, St. Petersburg, Russia, 65–85 (in Russian)

Dulnev, G. N., Zarichnyak, U. P. and Muratova, B. L. 1968. Heat transfer conductivity of fiber systems, (in Russian). *Heat Mass Transfer*, **7**, 82–89

Haffner, H. 1970. *Bundesminist.f.Bildungu.Wiss.*, BMBW-FB K 70-24

Nikayama, V., Daikoku, T. and Kuvahara, H. 1980. Dynamic model of enhanced boiling heat transfer on porous surface, Experimental investigation. *J. Heat Transfer*, **102**, 62–69

Semena, M. G., Gershuni, A. I. and Zaripov, V. K. 1984. *Thermal Tubes with Fibermetal Porous Structures*. Vishtcha Shcola, Kiev, Ukraine, 46–83 (in Russian)

Semena, M. G., Kravets, I. U., Fridrihson, U. V. and Brik, D. G. 1992. Investigation of pressure effect on boiling heat transfer performance of porous coated surfaces, (in Russian). *Proc. 2nd Minsk Int. Forum*, **4**, 59–62

Tikhonov, A. V. and Zaporozhtchenko, O. E. 1984. Boiling heat transfer of R113 on fibermetal coatings. *In Cryogenics and Conditioning. Investigation and Improving of Processes and Apparatus. Interinstitute Collected Volume of Scientific Papers*. LTIHP, St. Petersburg, Russia, 104–109 (in Russian)